

1 **Simple rules govern the diversity of bacterial nicotianamine-like metallophores**

2 Clémentine Laffont¹, Catherine Brutesco¹, Christine Hajjar¹, Gregorio Cullia², Roberto Fanelli²,
3 Laurent Ouerdane³, Florine Cavelier², Pascal Arnoux^{1,*}

4 ¹Aix Marseille Univ, CEA, CNRS, BIAM, Saint Paul-Lez-Durance, France F-13108.

5 ²Institut des Biomolécules Max Mousseron, IBMM, UMR-5247, CNRS, Université Montpellier,
6 ENSCM, Place Eugène Bataillon, 34095 Montpellier cedex 5, France.

7 ³CNRS-UPPA, Laboratoire de Chimie Analytique Bio-inorganique et Environnement, UMR 5254,
8 Hélioparc, 2, Av. Angot 64053 Pau, France.

9 ***Correspondance:** Pascal Arnoux, Aix Marseille Univ, CEA, CNRS, BIAM, Saint Paul-Lez-
10 Durance, France F-13108; pascal.arnoux@cea.fr; Tel. 04-42-25-35-70

11 **Keywords:** opine/opaline dehydrogenase, CntM, nicotianamine-like metallophore, bacillopaline

13 **ABSTRACT**

14 In metal-scarce environments, some pathogenic bacteria produce opine-type metallophores
15 mainly to face the host's nutritional immunity. This is the case of staphylopine, pseudopaline and
16 yersinopine, identified in *Staphylococcus aureus*, *Pseudomonas aeruginosa* and *Yersinia pestis*
17 respectively. These metallophores are synthesized by two (CntLM) or three enzymes (CntKLM),
18 CntM catalyzing the last step of biosynthesis using diverse substrates (pyruvate or α -ketoglutarate),
19 pathway intermediates (xNA or yNA) and cofactors (NADH or NADPH), depending on the species.
20 Here, we explored substrate specificity of CntM by combining bioinformatics and structural analysis
21 with chemical synthesis and enzymatic studies. We found that NAD(P)H selectivity was mainly due to
22 the amino acid at position 33 (*S. aureus* numbering) which ensures a preferential binding to NADPH
23 when it is an arginine. Moreover, whereas CntM from *P. aeruginosa* preferentially uses yNA over
24 xNA, the staphylococcal enzyme is not stereospecific. Most importantly, selectivity towards α -
25 ketoacids is largely governed by a single residue at position 150 of CntM (*S. aureus* numbering): an
26 aspartate at this position ensures selectivity towards pyruvate whereas an alanine leads to the
27 consumption of both pyruvate and α -ketoglutarate. Modifying this residue in *P. aeruginosa* led to a
28 complete reversal of selectivity. Thus, opine-type metallophore diversity is mainly mediated by the
29 absence/presence of a *cntK* gene encoding a histidine racemase, and the presence of an
30 aspartate/alanine at position 150 of CntM. These two simple rules predict the production of a fourth
31 metallophore by *Paenibacillus mucilaginosus*, which was confirmed *in vitro* and called bacillopaline.

34 **INTRODUCTION**

35 In metal-scarce environments, bacteria have to use efficient mechanisms for the uptake of
36 metals required for their growth. This is particularly the case for pathogenic bacteria that have to
37 confront the host's immune system. Indeed, the so-called "nutritional immunity" induces an additional
38 metal limitation by sequestering iron, zinc or manganese to prevent bacterial growth [1–4]. To face
39 this metal restriction, bacteria have developed metallophores to recover metals. In this context,
40 nicotianamine-like metallophores have been identified in some bacteria as playing an important role in
41 metal acquisition strategies. Staphylopine, pseudopaline and yersinopine are the three examples

42 currently known and recently identified in *S. aureus* [5], *P. aeruginosa* [6,7] and *Y. pestis* [8]
43 respectively. The biosynthesis of these nicotianamine-like metallophores occurs in two or three steps
44 depending on the species. When it is present, as in *S. aureus*, CntK, a histidine racemase, transforms
45 L-histidine (L-His) into D-histidine (D-His). CntL, a nicotianamine synthase-like, adds an
46 aminobutyrate moiety coming from S-adenosyl methionine (SAM) on the amino group of the substrate
47 (L-His in *P. aeruginosa* and *Y. pestis* or D-His in *S. aureus*) to form a pathway intermediate (yNA
48 with L-His or xNA with D-His). Finally, CntM, an enzyme belonging to the opine dehydrogenase
49 family, condenses the pathway intermediate with an α -ketoacid (pyruvate in the case of *S. aureus* and
50 *Y. pestis* or α -ketoglutarate (α KG) in the case of *P. aeruginosa*) using NAD(P)H to form an opine-type
51 metallophore (Figure 1).

52 Opine dehydrogenase catalyzes the NAD(P)H-dependent reductive condensation of the amino
53 group of an amino acid with an α -ketoacid to produce an N-(carboxyalkyl) amino acid, also known as
54 an opine, which exhibits either (L,L) or (D,L) stereochemistry [9]. The variety of amino acids and α -
55 ketoacids that can be used as substrates by opine dehydrogenases results in diverse products. For
56 example, the octopine dehydrogenase catalyzes the production of octopine, lysopine or histopine *via*
57 reductive condensation of pyruvate and L-arginine, L-lysine and L-histidine respectively [10–13].
58 Leucinopine, asparaginopine and glutaminopine are other examples of opines produced *via* reductive
59 condensation of α -ketoglutarate with L-leucine, L-asparagine and L-glutamine respectively [14,15]. In
60 addition to the diversity of substrates, opine dehydrogenases are also distinguished by their biological
61 roles. Indeed, in some marine invertebrates, opine dehydrogenases participate in the anaerobic
62 metabolism by insuring the last step of anaerobic glycolysis pathway therefore participating in the
63 propelling of these animals [16,17]. In plants, diverse opines are found inside crown gall tumors (for
64 example nopaline, agropine, octopine, mannopine or D-L and L-L-succinamopine) that are induced by
65 plant pathogenic bacteria as *Agrobacterium tumifaciens* [18]. In this case, the opines serve as nutrients
66 conferring selective growth advantages to the opine-producing and opine-utilizing microorganisms
67 [19,20].

68 Opine dehydrogenases are also involved in the biosynthesis of nicotianamine-like
69 metallophores in bacteria and their substrate specificity results in the production of diverse
70 metallophores. The activity of these opine dehydrogenases from *S. aureus*, *P. aeruginosa* and *Y. pestis*
71 (respectively called SaCntM, PaCntM and YpCntM) has been described: SaCntM uses NADPH and
72 pyruvate with xNA to produce staphylopin [5], YpCntM uses pyruvate and NADPH with yNA to
73 produce yersinopine [8], and PaCntM uses NAD(P)H and α -ketoglutarate with yNA to produce
74 pseudopaline [6,7]. Therefore, substrate specificity (and eventually stereospecificity in the case of
75 xNA *vs* yNA) of CntM leads to the production of diverse opine-type metallophores. These
76 metallophores are involved in metal acquisition, with metal specificity depending on the growth
77 medium. Staphylopin could transport copper, nickel, cobalt, zinc and iron [5,21,22], and participates
78 in zinc uptake in zinc-scarce environments [21,23]. Pseudopaline is involved in nickel uptake in
79 minimal media, whereas it is responsible for zinc uptake in zinc-scarce environment [6,24]. For both
80 *S. aureus* and *P. aeruginosa*, literature reports a link between the production of opine-type
81 metallophores and bacterial infection. For example, in *S. aureus*, the staphylopin receptor CntA plays
82 an important role in the optimal functioning of the urease activity and in the virulence: deletion of this
83 substrate binding protein leads to a decrease of murine bacteremia and urinary tract infections [22]. In
84 *P. aeruginosa*, transcriptomic analyses showed that the biosynthetic genes for pseudopaline are
85 overexpressed in burn wound infections in humans [25]. This overexpression would allow bypassing
86 metal limitations set up during nutritional immunity. Moreover, the pseudopaline's exporter CntI plays
87 an important role in the survival and growth of *P. aeruginosa* in cystic fibrosis airway: deletion of this
88 exporter results in an attenuation of this respiratory infection [26]. Similarly, the exporter of
89 staphylopin was found to be important for fitness in abscesses, even before staphylopin discovery

90 [27]. Concerning *Y. pestis*, no data indicates a link between yersinopine production and virulence at
91 this time and the discovery of this metallophore is so far restricted to *in vitro* studies [8].

92 In an effort to understand bacterial opine-type metallophore diversity, we studied substrate
93 specificity of CntM in *S. aureus* and *P. aeruginosa* by combining bioinformatic and structural analyses
94 with chemical synthesis and enzymatic studies. A single amino acid residue is responsible for the
95 preferential binding of NADPH, and a single residue is involved in the specificity towards pyruvate or
96 α -ketoglutarate. These simple rules in substrate specificity prompted us to dig into available genomes
97 for a bacteria possessing a *cntK* homologue together with a *cntM* gene predicted to use α -ketoglutarate.
98 This research ultimately led to the discovery of a new opine-type metallophore called bacillopaline in
99 *Paenibacillus mucilaginosus*.

100

101 MATERIALS AND METHODS

102 Bioinformatic analyses

103 SaCntM (*sav2468*) protein sequence was analyzed by searching for homologues using Psi-
104 BLAST search [28] through the NCBI databases (National Center for Biotechnology Information,
105 Bethesda, Maryland, USA) and the Pfam database (European Bioinformatics Institute, Hinxton,
106 England, UK). Sequence alignment was done using the Muscle program [29] with defaults criteria
107 from Jalview (version 2.10.3) [30]. Residues were colored following the Clustal coloring scheme with
108 intensity modified by a conservation color increment of 30%. Gene synteny were inspected using the
109 MaGe MicroScope web interface [31] added to sequence alignment analysis.

110 Cloning, expression and purification of proteins

111 The gene encoding the SaCntM protein (*sav2468*) was cloned in pET-SUMO and pET-101,
112 and the one encoding the PaCntM protein (*pa4835*) was cloned in pET-TEV according to standard
113 protocols. Similarly, the genes encoding the PmCntL and PmCntM proteins were cloned in pET-TEV
114 from genomic DNA. The primers used for these constructions are listed in Table S1. After co-
115 transformation with plasmid pRARE (encoding for rare codon in *E. coli*), *E. coli* BL21 strains were
116 aerobically cultivated with horizontal shaking in LB media supplemented with appropriate antibiotics
117 (kanamycin at 50 $\mu\text{g}\cdot\text{mL}^{-1}$ for pET-SUMO and pET-TEV, ampicillin at 50 $\mu\text{g}\cdot\text{mL}^{-1}$ for pET-101 and
118 chloramphenicol at 25 $\mu\text{g}\cdot\text{mL}^{-1}$ for pRARE). These strains were grown in diverse conditions (37°C or
119 16°C, with or without induction of protein expression by addition of 0.1 mM IPTG when the OD of
120 the culture was about 0.6; Table S2). After overnight growth, cells were recovered by centrifugation at
121 5,000 g for 20 min at 4°C. Cells were resuspended in buffer A and disrupted using a Constant cell
122 disruption system operating at 1.9 Kbar. Cell debris were removed by centrifugation at 8,000 g for 20
123 min. The supernatant was centrifuged at 100,000 g for 45 min at 4°C to remove cell wall debris and
124 membrane proteins. The resulting soluble fraction was purified by batch using a nickel-charged affinity
125 resin (Ni-NTA Agarose resin, ThermoFisher Scientific). The proteins were eluted stepwise with
126 imidazole (15 mM wash, 250 mM or 500 mM elution). Collected fractions were transferred into
127 imidazole-free buffer B (see Table S2 for details on the buffers used).

128 Site directed mutagenesis

129 Site directed mutagenesis were performed according to standard protocol from the
130 QuickChange II Site-Directed Mutagenesis kit (Agilent Technologies). The only difference was that *E.*
131 *coli* DH10 β Competent Cells were used instead of XL1-Blue Supercompetent Cells for
132 transformations. Selection of colonies was done after spreading on LB plate supplemented with
133 appropriate antibiotics. Plasmid pET-SUMO containing the gene encoding the SaCntM protein and

134 plasmid pET-TEV containing the gene encoding the PaCntM protein were used as mutagenesis
135 templates for the D150A and A153D substitutions respectively. For the R33H substitution from
136 SaCntM, mutagenesis was performed from plasmid pET-101 containing the gene encoding the
137 SaCntM protein as template. Primer pairs were designed for single substitutions and were then
138 synthesized by Eurofins Genomics (Table S1).

139 **Chemical synthesis of xNA and yNA**

140 The chemical synthesis of xNA has recently been described [32]. The same strategy was used
141 for the chemical synthesis of yNA, although L-His-OMe was used instead of D-His-OMe as starting
142 material. Purified intermediates and their characterization are described in the supplementary
143 materials.

144 **CntM activity assay**

145 Enzymatic reactions of CntM were performed at 28°C in microplates and with purified
146 proteins. They were carried out in a reaction volume of 100 µL in buffer C (50 mM BisTrisPropane,
147 100 mM NaCl, pH = 7 for SaCntM and PmCntM or pH = 8 for PaCntM) containing 2 or 5 µg of
148 enzyme, 0.2 mM of NADH or NADPH (Sigma-Aldrich), 0.2 mM of xNA or yNA (chemically
149 synthesized), and 1 mM of pyruvate or α-ketoglutarate (Sigma-Aldrich), unless otherwise stated. The
150 absorbance at 340 nm was measured using a microplate reader (Infinite 200 Pro; Tecan) to follow the
151 oxidation of NADPH illustrating the progress of the reaction. Activities were calculated from the
152 initial rate and the amount of enzyme used. Kinetic parameters were estimated according to the
153 Michaelis-Menten kinetic without (1) or with the substrate inhibition model (2) using SigmaPlot.
154 These values were used to plot a fit on the experimental data. (V_m : Maximum velocity; K_m : Michaelis
155 constant; [S]: substrate concentration; K_i : Inhibition constant).

156
$$(1): v = \frac{v_m [S]}{K_m + [S]}$$

157
$$(2): v = \frac{v_m [S]}{K_m + [S] \left(1 + \frac{[S]}{K_i}\right)}$$

158

159 **Fluorescence resonance energy transfer (FRET) studies**

160 Fluorescence studies were performed using a Cary Eclipse spectrophotometer (Agilent). The
161 FRET experiment was done using a protein concentration of 5 µM and an excitation wavelength at
162 280 nm (tryptophan excitation). The emission at 340nm was transferred to the NAD(P)H and the
163 signal was recorded between 400 and 500 nm. Five spectra were averaged in order to increase signal
164 to noise ratio.

165 **Activity assay followed by TLC**

166 The assay consisted in incubating the purified enzymes at a final concentration of 2.5 µM and
167 using carboxyl-¹⁴C]-labeled SAM (2.5 µM), NADPH or NADH (30 µM), L- or D-histidine (10 µM)
168 and α-keto acid (pyruvate or α-ketoglutarate; 1mM). The total volume was 100 µL in buffer D (50 mM
169 of HEPES, 1 mM of DTT, 1mM of EDTA, pH = 9). The mixtures were incubated for 30 min at 28 °C.
170 The reactions were stopped by adding ethanol to a final concentration of 50 % (v/v) and the products
171 were then separated by thin layer chromatography. An aliquot of 10 µL of the reaction mixtures were
172 spotted on HPTLC (High Performance TLC) Silica Gel 60 Glass Plates (Merck KGaA), and the plates
173 were developed with a phenol:n-butanol:formate:water (12:3:2:3 v/v) solvent system. These separation
174 parameters were used in the initial biochemical characterization of plant nicotianamine synthase [33]
175 and of staphylopin and pseudopaline [5,6]. HPTLC plates were dried and exposed to a ¹⁴C]-sensitive

176 imaging plate for one day. Imaging plates were then scanned on a Typhoon FLA 7000
177 phosphorimager (GE Healthcare).

178

179 **Cell culture conditions of *Paenibacillus mucilaginosus***

180 *Paenibacillus mucilaginosus*, sub sp. 1480D (from Collection DSMZ) was grown by
181 inoculating stock bacteria into 20 mL sterile medium (TSB 1/10) at 30°C for 48h. Genomic DNA was
182 extracted using the protocols and pretreatments for Gram-positive bacteria from DNeasy Blood and
183 Tissue kit (Qiagen).

184

185 **RESULTS AND DISCUSSION**

186 **Specificity towards NADH or NADPH**

187 The structure of CntM have been solved in a binary/tertiary complex with NADPH or NADPH
188 and xNA, revealing the residues that are involved in the complex formation and building the active
189 site [8,32]. First focusing on the NADPH binding site of SaCntM (Figure 2A) we observed that the
190 phosphate group of NADPH is sandwiched by the side chains of two positively charged residues (R33
191 and K39) that are rather conserved in the CntM family. However, a sequence alignment of CntM from
192 nine different species including *S. aureus*, *P. aeruginosa* and *Y. pestis* shows that R33 residue in
193 SaCntM (also present in sequence from *Y. pestis*) is replaced by a histidine in PaCntM (Figure 2B).
194 Because it is known that SaCntM and YpCntM specifically uses NADPH [5,8] while PaCntM could
195 use NADH or NADPH depending on the conditions [6–8], we hypothesized that the nature of the
196 amino acid residue at this position could determine the NADH/NADPH selectivity by CntM.

197 We therefore sought to determine the role of this residue in NAD(P)H selectivity by replacing
198 this arginine by a histidine in a SaCntM:R33H variant. Because the histidine could either be neutral or
199 positively charged at pH above or below its pK_a , the binding of NAD(P)H was followed at two pHs
200 (6.0 and 8.5). We found that the WT enzyme, whatever the pH, still preferentially binds NADPH over
201 NADH (Figure 3). On the contrary, the R33H mutant behaves as the WT at pH 6.0, whereas it loses its
202 preferential binding property at a higher pH. This shows that a histidine at this position could serve as
203 a selective residue, stabilizing NADPH at acidic pH when the imidazole ring of histidine is positively
204 charged, and favoring NADH binding when histidine is neutral at basic pH, overall explaining the
205 difference of selectivity in the literature [6–8]. Interestingly, we noted that *Fictibacillus arsenicus*
206 possesses a histidine residue at the conserved position equivalent to K39 in *S. aureus*, suggesting the
207 same possibility of preferential NADH binding at basic pH.

208 **Specificity towards xNA or yNA**

209 *In vivo*, CntM uses the product of CntL *i.e.* xNA or yNA depending on the species. However,
210 using enzymatically produced xNA or yNA, McFarlane *et al.* (2018) suggested that SaCntM could use
211 both diastereoisomers. Activities from *S. aureus* (SaCntM) and from *P. aeruginosa* (PaCntM) were
212 therefore compared for their ability to use chemically synthesized xNA and yNA as substrate (Figure
213 4). The chemical synthesis of xNA was recently reported [32] and we were able to synthesize yNA by
214 following the same approaches (see the experimental procedures and the supplementary materials).
215 Reactions were then performed *in vitro* using purified proteins and a concentration range of xNA and
216 yNA with a fixed concentration of other substrates: 0.2 mM of NADPH and 1 mM of pyruvate (when
217 evaluating SaCntM) or α -ketoglutarate (when evaluating PaCntM). Overall, we found that the activity
218 of CntM from *S. aureus* and *P. aeruginosa* towards yNA and xNA were different. In the case of
219 SaCntM, although xNA is used *in vivo* to produce staphylopine, its activity is higher when using yNA
220 *in vitro*. Indeed, the k_{cat} for the reaction with yNA is ~2-fold higher than the one with xNA (3.18 s⁻¹
221 and 1.67 s⁻¹ respectively). However, the K_m for the reaction with yNA is ~2-fold higher than the one

222 with xNA (47 μM and 23 μM respectively), leading to a catalytic efficiency ($k_{\text{cat}}/K_{\text{m}}$) of the same order
223 of magnitude for the two substrates (Table 1). In the case of PaCntM, the enzyme uses yNA to
224 produce pseudopaline *in vivo*. In agreement with this, we found that the reaction with yNA is more
225 efficient than the one with xNA, the reaction with yNA exhibiting a catalytic efficiency ~ 10 -fold
226 higher than with xNA (29 618 $\text{M}^{-1}\text{s}^{-1}$ and 2 918 $\text{M}^{-1}\text{s}^{-1}$ respectively).

227 In the past decades, several opine dehydrogenases have been studied and their biosynthetic
228 reactions generally exhibit a substrate stereospecificity towards the amino group with most enzymes
229 using the L-stereoisomer as substrate [9]. For example, substrate stereospecificity has been outlined
230 for the octopine dehydrogenase from *Pecten maximus* [12] and the structure of this enzyme shows a
231 negatively charged cavity acting as a “charge ruler”, which favors L-arginine binding. Here, we found
232 that even if SaCntM uses xNA *in vivo*, it is also capable of using yNA *in vitro*. This trend confirms the
233 one outlined by McFarlane *et al.* [8] using enzymes from different species. Under their experimental
234 conditions, PaCntM exhibited a k_{cat} of 0.016 s^{-1} in the presence of xNA, which was biosynthesized
235 with SaCntL. Accordingly, we found that PaCntM preferentially used yNA whether *in vitro* or *in vivo*.
236 All these data therefore suggest that there is a substrate stereospecificity in the case of PaCntM, which
237 is not found in SaCntM. We further noted that, using yNA but not xNA, a drop in enzyme activity is
238 visible at high substrate concentrations, which suggests a mechanism of substrate inhibition (Figure 4).
239 Indeed, the fits made with a substrate inhibition model added to the Michaelis-Menten kinetic better
240 cover the experimental data (Figure 4; plain lines). However, this substrate inhibition is not visible
241 when using xNA as substrate.

242 **Specificity towards pyruvate or α -ketoglutarate**

243 In order to find amino acid residues involved in the pyruvate/ α -ketoglutarate selectivity by
244 CntM, we searched for residues located in the vicinity of the active site (*i.e.* the nicotinamide moiety)
245 and conserved in species known to use pyruvate (*S. aureus* and *Y. pestis*) but differing in species
246 known to use α -ketoglutarate (*P. aeruginosa*). This pointed to the aspartic acid residue at position 150
247 in SaCntM, which is also present in YpCntM but replaced by an alanine in PaCntM (corresponding to
248 residue 153 in this enzyme). We hypothesized that the nature of the amino acid residue at this position
249 would determine the pyruvate/ α -ketoglutarate selectivity by CntM. This postulate was also proposed
250 by McFarlane *et al.* [8]. In order to test the role of this amino acid in pyruvate/ α -ketoglutarate
251 selectivity, we replaced the aspartic acid by an alanine in SaCntM (D150A variant) and did the
252 opposite mutation in PaCntM (A153D). The activities of these proteins were then compared for their
253 ability to use of pyruvate and α -ketoglutarate as substrates (Figure 5). The reactions were performed
254 using a concentration range of pyruvate and α -ketoglutarate with a fixed concentration of others
255 substrates: 0.2 mM of NAD(P)H and 0.2 mM of xNA (when using SaCntM) or yNA (PaCntM). As a
256 control, we verified that the mutation did not affect the binding of the NADPH on SaCntM (Figure
257 S8).

258 With regard to SaCntM, we confirmed that the WT was only able to use pyruvate, with a k_{cat}
259 of 1.0 s^{-1} and a K_{m} of 51 μM , resulting in a catalytic efficiency of 19 592 $\text{M}^{-1}\text{s}^{-1}$ (Figure 5 and Table 2).
260 On the contrary, the D150A variant of SaCntM could use both pyruvate and α -ketoglutarate as
261 substrates. Indeed, although the maximum activity is not reached within the concentration range
262 tested, the kinetic parameters calculated for both pyruvate and α -ketoglutarate are in the same order of
263 magnitude. This single substitution therefore led to a decreased activity when using pyruvate but most
264 of all, significantly increased the activity when using α -ketoglutarate. Even if we take a lower limit for
265 the k_{cat} of 1.65 s^{-1} for α -ketoglutarate, this would correspond to a more than 40-fold increased as
266 compared to the WT SaCntM. We then investigated whether the opposite mutation in PaCntM would
267 trigger the same effect on substrate selectivity. Here again, we confirmed that the WT enzyme could
268 only use α -ketoglutarate with a k_{cat} of 0.27 s^{-1} and a K_{m} of 133 μM . Strikingly, we found that the

269 A153D substitution in PaCntM led to a complete reversal of selectivity, with the variant only being
270 able to use pyruvate and unable to use α -ketoglutarate anymore. This mutation is indeed accompanied
271 by a more than 20-fold increase in k_{cat} for pyruvate and \sim 30-fold decrease for α -ketoglutarate, *i.e.* a
272 complete switch in substrate specificity. Consequently, substrate specificity of CntM towards pyruvate
273 or α -ketoglutarate is mainly governed by this single amino acid (position 150 in SaCntM or 153 in
274 PaCntM): an aspartate ensures the selection of pyruvate whereas an alanine leads to α -ketoglutarate
275 specificity. To our knowledge, this is the first example showing that substrate specificity might be
276 tuned in opine/opaline dehydrogenases family. There are however some examples of redesigned
277 substrate specificity in dehydrogenases such as the production of a highly active malate
278 dehydrogenase starting from lactate dehydrogenase [34]. In this case, the Gln102Arg mutation of
279 *Bacillus stearothermophilus* lactate dehydrogenase led to a shift in k_{cat}/K_m with malate so that it equal
280 that of native lactate dehydrogenase for its natural substrate. Examples of site directed mutagenesis
281 studies in the opine/opaline family were centered on the catalytic residues and all led to decreased
282 activities towards substrates and none explored the putative α -ketoacid specificity [12,35].

283 **Identification of a novel nicotianamine-like metallophore**

284 Having established the molecular determinant for the α -ketoacid selectivity of CntM, we have
285 proposed simple rules governing the production of nicotianamine-like metallophores: 1-) the presence
286 or absence of a *cntK* homologue leads to the production of D- or L-His respectively (then used by
287 CntL to produce xNA or yNA respectively), and 2-) the presence of an aspartate or an alanine at
288 position 150 (*S. aureus* numbering) results in pyruvate or α -ketoglutarate incorporation, respectively.
289 Applying these rules, we searched for a species capable of producing the missing variant, which would
290 use xNA and α -ketoglutarate, *i.e.* a species possessing a *cntK* homologue and an alanine at position
291 responsible for α -ketoglutarate selectivity. Digging into available genomes *in silico*, we identified
292 *Paenibacillus mucilaginosus* as a good candidate. Indeed, this species carries an A153 in CntM (as *P.*
293 *aeruginosa*) and possess a *cntK* in its *cnt* operon (as *S. aureus*) (Figure 2B-C).

294 To check the validity of this hypothesis, genes encoding the CntL and CntM from *P.*
295 *mucilaginosus* (PmCntL and PmCntM respectively) were amplified from genomic DNA, cloned in
296 expression vectors, purified and used to determine the substrates they consumed *in vitro* (Figure 6).
297 We then assayed enzyme activities using TLC separation and using carboxyl- 14 C]-labeled SAM. In
298 the TLC assay, 14 C]-labeled SAM shows a characteristic profile with one strong band and two others
299 bands of much lower intensity (Figure 6 A). The incubation of 14 C]-labeled SAM with PmCntL led to
300 another prominent band in the presence of D-His, which is not found using L-His. This novel band,
301 migrating below the SAM band, corresponds to the xNA intermediate. This indicates that PmCntL
302 uses D-His and not L-His, and further confirms the link between the presence of a *cntK* gene and the
303 use of D-His by CntL. We then tested the substrate specificity of PmCntM by co-incubating both
304 PmCntL and PmCntM together with diverse substrates: pyruvate or α -ketoglutarate with NADH or
305 NADPH. When using NADPH and D-His with either pyruvate or α -ketoglutarate, we neither detected
306 the SAM nor xNA pattern, but found a novel band migrating just above the SAM in the presence of
307 pyruvate (which corresponds to staphylopine) and just below the SAM in the presence of α -
308 ketoglutarate. Surprisingly, we thus found that PmCntM could use both pyruvate and α -ketoglutarate
309 in this TLC assay. However, TLC experiments were run using a defined incubation time (30 min),
310 which might hinder differences in enzyme efficiency. We therefore determined the enzymatic
311 parameters of PmCntM using the purified protein and a concentration range of pyruvate and α -
312 ketoglutarate with a fixed concentration of others substrates: 0.2 mM of NADPH and 0.2 mM of xNA
313 (Figure 6 B). We found that the catalytic efficiency is 10-fold better for α -ketoglutarate than for
314 pyruvate ($10\,367\text{ M}^{-1}\text{s}^{-1}$ and $1\,016\text{ M}^{-1}\text{s}^{-1}$ respectively; Table 3). These data therefore suggest that our
315 hypothesis is valid: CntL and CntM from *P. mucilaginosus* produce an additional variant of opine-type

316 metallophore with D-His, NADPH and α -ketoglutarate. This metallophore has been called
317 bacillopaline as it belongs to the opaline family (Figure 6 C). Moreover, we found that, in addition to
318 using both pyruvate and α -ketoglutarate, CntM from *P. mucilaginosus* is also able to use both xNA
319 and yNA (Figure S9, Table S3). Contrary to human pathogens like *S. aureus*, *P. aeruginosa* or *Y.*
320 *pestis* in which opine-type metallophores were discovered [5–8], *P. mucilaginosus* is a soil bacteria.
321 The production of opine-type metallophores was shown to be regulated by zinc through the zur (zinc
322 uptake repressor) repressor [6,23], which is likely the case in *P. mucilaginosus*. Therefore, a possible
323 hypothesis is that bacillopaline production could be induced in calcareous soils where zinc
324 bioavailability was shown to be low [37]. In the past decade, *P. mucilaginosus* have been studied for
325 its capacity in wastewater treatment, but also as biofertilizer and plant growth promoting rhizobacteria
326 [38–40]. Indeed, in addition to producing biofloculants or plant hormones, this species is able to
327 solubilize phosphates, to fix nitrogen and to produce ammonia. Moreover, it is able to produce
328 siderophores, which contributes to plant growth by indirectly preventing the growth of plant pathogens
329 [39,41]. Similarly, we could hypothesize that bacillopaline could contribute in the same way to
330 maintain plant homeostasis.

331 In conclusion, studying the substrate specificity of the enzyme catalyzing the last step of the
332 biosynthesis of bacterial nicotianamine-like metallophores allowed us to determine simple rules
333 governing their production. First, the presence or absence of a *cntK* gene leads to the use of
334 respectively D-His or L-His by CntL resulting in the incorporation of respectively xNA or yNA by
335 CntM. Secondly, the presence of an aspartate or an alanine at position 150 on CntM (*S. aureus*
336 numbering) results in pyruvate or α -ketoglutarate incorporation, respectively. Thanks to these simple
337 rules, it is now possible to predict the nature of the nicotianamine-like metallophore produced by all
338 bacteria possessing a *cnt* operon in their genome.

339

340 **Acknowledgments**

341 We thank the Agence Nationale de la Recherche (grant ANR-14-CE09-0007-02) for initial support
342 and the association Vaincre la Mucoviscidose (VLM, grant RFI20160501495) for financial support.

343

344 **Conflict of Interest**

345 The authors declare that they have no conflicts of interest with the contents of this article.

346

347 **Author contributions**

348 C.L. and P.A. designed the experiments. C.L., C.B., C.H. and L.O. carried out the experiments. C.L.,
349 C.B. and P.A. analyzed the data. G.C, R.F synthesized xNA and yNA under the supervision of F.C.
350 C.L. and P.A. wrote the manuscript with contributions from F.C.

351

352 **References**

- 353 1 Capdevila, D. A., Wang, J. and Giedroc, D. P. (2016) Bacterial Strategies to Maintain Zinc
354 Metallostasis at the Host-Pathogen Interface. *J. Biol. Chem.* **291**, 20858–20868.
355 2 Hood, M. I. and Skaar, E. P. (2012) Nutritional immunity: transition metals at the pathogen–host
356 interface. *Nat. Rev. Microbiol.* **10**, 525–537.
357 3 Weinberg, E. D. (1975) Nutritional immunity. Host’s attempt to withhold iron from microbial
358 invaders. *JAMA* **231**, 39–41.
359 4 Zygiel, E. M. and Nolan, E. M. (2018) Transition Metal Sequestration by the Host-Defense
360 Protein Calprotectin. *Annu. Rev. Biochem.* **87**, 621–643.

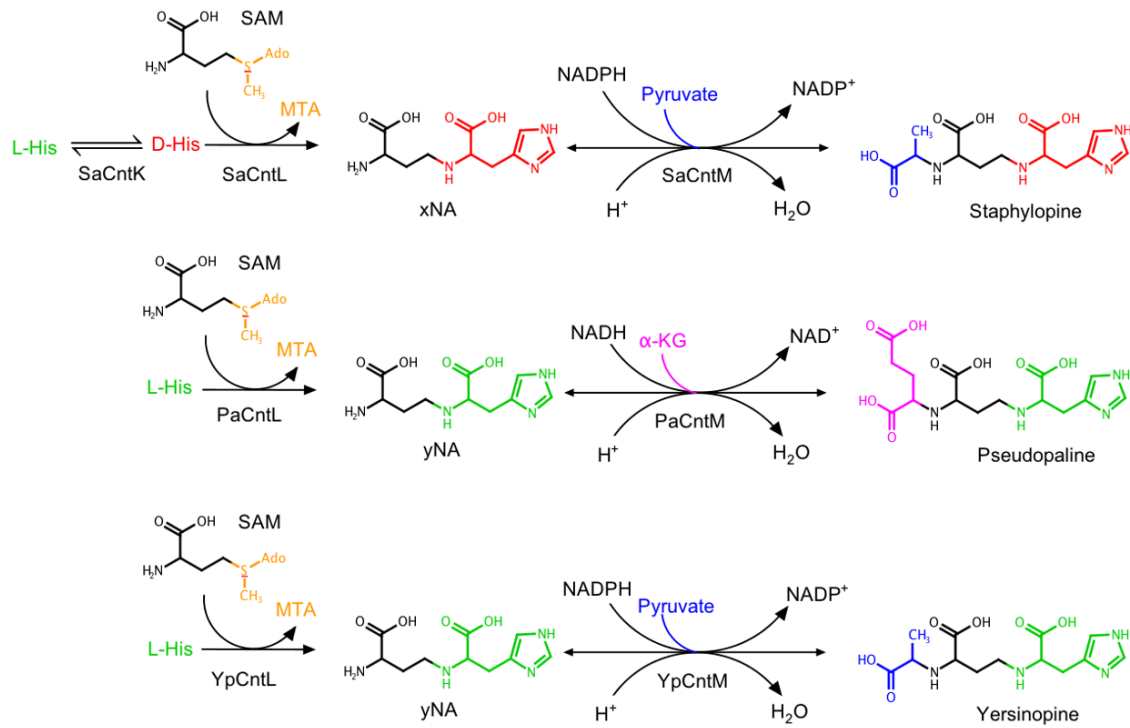
- 361 5 Ghsein, G., Brutesco, C., Ouerdane, L., Fojcik, C., Izaute, A., Wang, S., Hajjar, C., Lobinski, R.,
362 Lemaire, D., Richaud, P., et al. (2016) Biosynthesis of a broad-spectrum nicotianamine-like
363 metallophore in *Staphylococcus aureus*. *Science* **352**, 1105–1109.
- 364 6 Lhospice, S., Gomez, N. O., Ouerdane, L., Brutesco, C., Ghsein, G., Hajjar, C., Liratni, A.,
365 Wang, S., Richaud, P., Bleves, S., et al. (2017) *Pseudomonas aeruginosa* zinc uptake in chelating
366 environment is primarily mediated by the metallophore pseudopaline. *Sci. Rep.* **7**.
- 367 7 McFarlane, J. S. and Lamb, A. L. (2017) Biosynthesis of an Opine Metallophore by *Pseudomonas*
368 *aeruginosa*. *Biochemistry* **56**, 5967–5971.
- 369 8 McFarlane, J. S., Davis, C. L. and Lamb, A. L. (2018) Staphylopine, pseudopaline, and
370 yersinopine dehydrogenases: A structural and kinetic analysis of a new functional class of opine
371 dehydrogenase. *J. Biol. Chem.* **293**, 8009–8019.
- 372 9 Thompson, J. and Donkersloot, J. A. (1992) N-(Carboxyalkyl)Amino Acids: Occurrence,
373 Synthesis, and Functions. *Annu. Rev. Biochem.* **61**, 517–57.
- 374 10 Bates, H. A., Kaushal, A., Deng, P. N. and Sciaky, D. (1984) Structure and synthesis of histopine,
375 a histidine derivative produced by crown gall tumors. *Biochemistry* **23**, 3287–3290.
- 376 11 Biemann, K., Lioret, C., Asselineau, J., Lederer, E. and Polonsky, J. (1960) On the structure of
377 lysopine, a new amino acid isolated from crown gall tissue. *Biochim. Biophys. Acta* **40**, 369–370.
- 378 12 Smits, S. H. J., Mueller, A., Schmitt, L. and Grieshaber, M. K. (2008) A Structural Basis for
379 Substrate Selectivity and Stereoselectivity in Octopine Dehydrogenase from *Pecten maximus*. *J.*
380 *Mol. Biol.* **381**, 200–211.
- 381 13 Van Thoai, N., Huc, C., Pho, D. B. and Olomucki, A. (1969) Octopine déshydrogénase: \square :
382 Purification et Propriétés Catalytiques. *Biochim. Biophys. Acta BBA - Enzymol.* **191**, 46–57.
- 383 14 Chang, C.-C. and Chen, C.-M. (1983) Evidence for the presence of N^2 -(1,3-dicarboxypropyl)-L-
384 amino acids in crown-gall tumors induced by *Agrobacterium tumefaciens* strains 181 and EU6.
385 *FEBS Lett.* **162**, 432–435.
- 386 15 Chang, C.-C., Chen, C.-M., Adams, B. R. and Trost, B. M. (1983) Leucinopine, a characteristic
387 compound of some crown-gall tumors. *Proc. Natl. Acad. Sci. USA* **80**, 3573–3576.
- 388 16 Gäde, G., Weeda, E. and Gabbott, P. A. (1978) Changes in the Level of Octopine during the
389 Escape Responses of the Scallop, *Pecten maximus* (L.). *J. Comp. Physiol. B* **124**, 121–127.
- 390 17 Harcet, M., Perina, D. and Pleše, B. (2013) Opine Dehydrogenases in Marine Invertebrates.
391 *Biochem. Genet.* **51**, 666–676.
- 392 18 Moore, L. W., Chilton, W. S. and Canfield, M. L. (1997) Diversity of Opines and Opine-
393 Catabolizing Bacteria Isolated from Naturally Occurring Crown Gall Tumors. *Appl. Environ.*
394 *Microbiol.* **63**, 201–207.
- 395 19 Montoya, A. L. (1977) Octopine and Nopaline Metabolism in *Agrobacterium tumefaciens* and
396 Crown Gall Tumor Cells: Role of Plasmid Genes. *J. Bacteriol.* **129**, 101–107.
- 397 20 Tremblay, G., Gagliardo, R., Chilton, W. S. and Dion, P. (1987) Diversity among Opine-Utilizing
398 Bacteria: Identification of Coryneform Isolates. *Appl. Environ. Microbiol.* **53**, 1519–1524.
- 399 21 Grim, K. P., San Francisco, B., Radin, J. N., Brazel, E. B., Kelliher, J. L., Párraga Solórzano, P.
400 K., Kim, P. C., McDevitt, C. A. and Kehl-Fie, T. E. (2017) The Metallophore Staphylopine
401 Enables *Staphylococcus aureus* To Compete with the Host for Zinc and Overcome Nutritional
402 Immunity. *mBio* (Torres, V. J., ed.) **8**.
- 403 22 Remy, L., Carrière, M., Derré-Bobillot, A., Martini, C., Sanguinetti, M. and Borezée-Durant, E.
404 (2013) The *Staphylococcus aureus* Opp1 ABC transporter imports nickel and cobalt in zinc-
405 depleted conditions and contributes to virulence: Nickel and cobalt uptake in *Staphylococcus*
406 *aureus*. *Mol. Microbiol.* **87**, 730–743.
- 407 23 Fojcik, C., Arnoux, P., Ouerdane, L., Aigle, M., Alfonsi, L. and Borezée-Durant, E. (2018)
408 Independent and cooperative regulation of staphylopine biosynthesis and trafficking by Fur and
409 Zur: Regulation of *S. aureus cnt* operon by Fur and Zur. *Mol. Microbiol.* **108**, 159–177.
- 410 24 Mastropasqua, M. C., D’Orazio, M., Cerasi, M., Pacello, F., Gismondi, A., Canini, A., Canuti, L.,
411 Consalvo, A., Ciavardelli, D., Chirullo, B., et al. (2017) Growth of *Pseudomonas aeruginosa* in
412 zinc poor environments is promoted by a nicotianamine-related metallophore: Metallophore-
413 mediated zinc uptake in *Pseudomonas aeruginosa*. *Mol. Microbiol.* **106**, 543–561.
- 414 25 Bielecki, P., Puchałka, J., Wos-Oxley, M. L., Loessner, H., Glik, J., Kawecki, M., Nowak, M.,
415 Tümmler, B., Weiss, S. and dos Santos, V. A. P. M. (2011) In-Vivo Expression Profiling of

- 416 *Pseudomonas aeruginosa* Infections Reveals Niche-Specific and Strain-Independent
417 Transcriptional Programs. PLoS ONE (Brown, S. P., ed.) **6**, e24235.
- 418 26 Gi, M., Lee, K.-M., Kim, S. C., Yoon, J.-H., Yoon, S. S. and Choi, J. Y. (2015) A novel
419 siderophore system is essential for the growth of *Pseudomonas aeruginosa* in airway mucus. Sci.
420 Rep. **5**, 14644.
- 421 27 Ding, Y., Fu, Y., Lee, J. C. and Hooper, D. C. (2012) *Staphylococcus aureus* NorD, a Putative
422 Efflux Pump Coregulated with the Opp1 Oligopeptide Permease, Contributes Selectively to
423 Fitness *In Vivo*. J. Bacteriol. **194**, 6586–6593.
- 424 28 Altschul, S. F., Madden, T. L., Schäffer, A. A., Zhang, J., Zhang, Z., Miller, W. and Lipman, D. J.
425 (1997) Gapped BLAST and PSI-BLAST: a new generation of protein database search programs.
426 Nucleic Acids Res. **25**, 3389–3402.
- 427 29 Edgar, R. C. (2004) MUSCLE: multiple sequence alignment with high accuracy and high
428 throughput. Nucleic Acids Res. **32**, 1792–1797.
- 429 30 Clamp, M., Cuff, J., Searle, S. M. and Barton, G. J. (2004) The Jalview Java alignment editor.
430 Bioinformatics **20**, 426–427.
- 431 31 Vallenet, D., Belda, E., Calteau, A., Cruveiller, S., Engelen, S., Lajus, A., Le Fèvre, F., Longin,
432 C., Mornico, D., Roche, D., et al. (2013) MicroScope—an integrated microbial resource for the
433 curation and comparative analysis of genomic and metabolic data. Nucleic Acids Res. **41**, D636–
434 D647.
- 435 32 Hajjar, C., Fanelli, R., Laffont, C., Brutesco, C., Cullia, G., Tribout, M., Nurizzo, D., Borezée-
436 Durant, E., Voulhoux, R., Pignol, D., et al. (2019) Control by Metals of Staphylopine
437 Dehydrogenase Activity during Metallophore Biosynthesis. J. Am. Chem. Soc.
- 438 33 Higuchi, K., Kanazawa, K., Nishizawa, N.-K. and Mori, S. (1996) The role of nicotianamine
439 synthase in response to Fe nutrition status in Gramineae. Plant Soil **178**, 171–177.
- 440 34 Wilks, H. M., Hart, K. W., Feeney, R., Dunn, C. R., Muirhead, H., Chia, W. N., Barstow, D. A.,
441 Atkinson, T., Clarke, A. R. and Holbrook, J. J. (1988) A specific, highly active malate
442 dehydrogenase by redesign of a lactate dehydrogenase framework. Science **242**, 1541–1544.
- 443 35 Müller, A., Janßen, F. and Grieshaber, M. K. (2007) Putative reaction mechanism of
444 heterologously expressed octopine dehydrogenase from the great scallop, *Pecten maximus* (L).
445 FEBS J. **274**, 6329–6339.
- 446 36 Hu, X. F., Li, S. X., Wu, J. G., Wang, J. F., Fang, Q. L. and Chen, J. S. (2010) Transfer of
447 *Bacillus mucilaginosus* and *Bacillus edaphicus* to the genus *Paenibacillus* as *Paenibacillus*
448 *mucilaginosus* comb. nov. and *Paenibacillus edaphicus* comb. nov. Int. J. Syst. Evol. Microbiol.
449 **60**, 8–14.
- 450 37 Alloway, B. J. (2009) Soil factors associated with zinc deficiency in crops and humans. Environ.
451 Geochem. Health **31**, 537–548.
- 452 38 Deng, S., Bai, R., Hu, X. and Luo, Q. (2003) Characteristics of a bioflocculant produced by
453 *Bacillus mucilaginosus* and its use in starch wastewater treatment. Appl. Microbiol. Biotechnol.
454 **60**, 588–593.
- 455 39 Goswami, D., Parmar, S., Vaghela, H., Dhandhukia, P. and Thakker, J. N. (2015) Describing
456 *Paenibacillus mucilaginosus* strain N3 as an efficient plant growth promoting rhizobacteria
457 (PGPR). Cogent Food Agric. (Moral, M. T., ed.) **1**.
- 458 40 Liu, S., Tang, W., Yang, F., Meng, J., Chen, W. and Li, X. (2017) Influence of biochar application
459 on potassium-solubilizing *Bacillus mucilaginosus* as potential biofertilizer. Prep. Biochem.
460 Biotechnol. **47**, 32–37.
- 461 41 Haas, D. and Défago, G. (2005) Biological control of soil-borne pathogens by fluorescent
462 *pseudomonads*. Nat. Rev. Microbiol. **3**, 307–319.
- 463 42 Lenz, M., Fademrecht, S., Sharma, M., Pleiss, J., Grogan, G. and Nestl, B. M. (2018) New imine-
464 reducing enzymes from β -hydroxyacid dehydrogenases by single amino acid substitutions.
465 Protein Eng. Des. Sel. **31**, 109–120.
- 466
- 467
- 468

469 **Figures and figure legends**

470

471

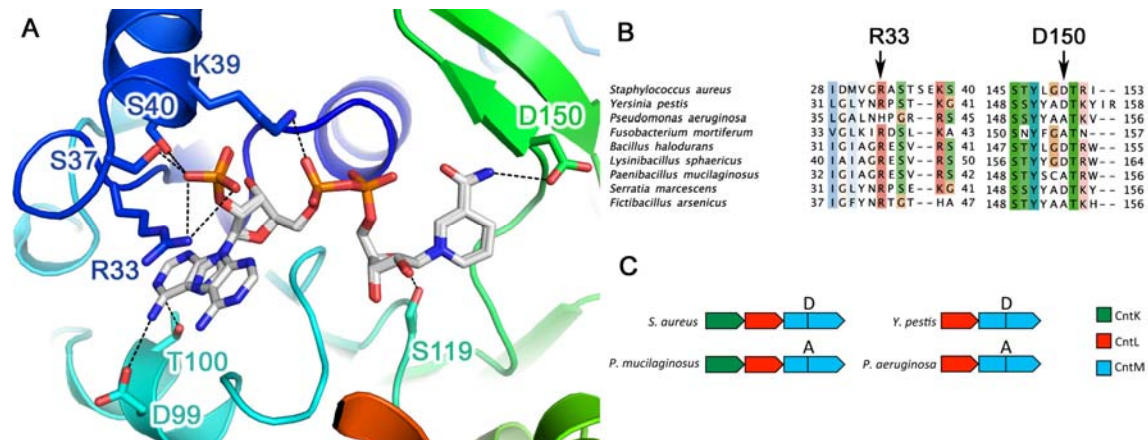


472

473 Figure 1: Differences in the staphylopinine, pseudopaline, and yersinopine biosynthetic pathways.

474 Adapted from [5,6,8].

475



476

477

478 Figure 2: CntM structure, sequence conservation around NADPH and operon diversity highlight

479 protein selectivity. (A) Details of the NADPH binding site on SaCntM with side chains of residues

480 located up to 4Å around the NADPH represented in stick. The protein is colored from N-terminus

481 (blue) to C-terminus (red). (B) Sequence alignment of nine CntM protein sequences from bacteria.

482 Threshold for the Clustal coloring scheme correspond to 30 % sequence conservation as defined in

483 Jalview. Arrows point to residues involved in NADPH/NADH selectivity and pyruvate/ α -ketoglutarate

484 selectivity. (C) Genomic organization of the biosynthetic genes of four different *cnt* operons in

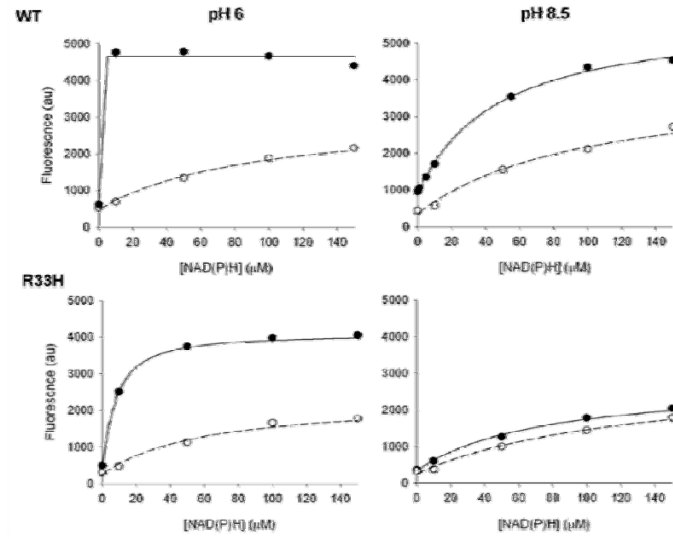
485

486

487

488

489

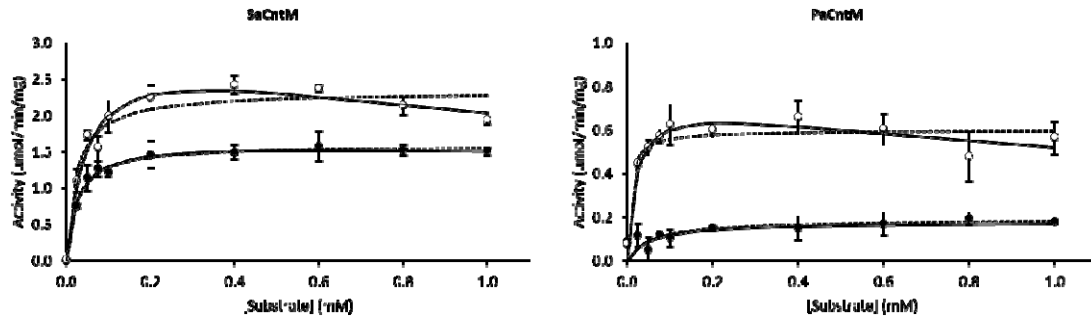


487

488 Figure 3: Titration of NADPH (black circles) and NADH (white circles) binding to SaCntM (5 μM) at
489 pH = 6.0 or pH = 8.5 followed by fluorescence energy transfer between tryptophan excitation (280
490 nm) and NAD(P)H emission (450 nm).

491

492



493

494 Figure 4: Activity profile of SaCntM and PaCntM using variable concentrations of xNA (black circle)
495 and yNA (white circle) with fixed concentrations of other substrates: 0.2 mM of NADPH and 1 mM of
496 pyruvate when evaluating SaCntM, or 0.2 mM of NADH and 1 mM of α -ketoglutarate when
497 evaluating PaCntM. The data points are means of three replicates with standard deviations. The fits are
498 made using the Michaelis-Menten model considering (continuous line) or not (dashed line) a substrate
499 inhibition.

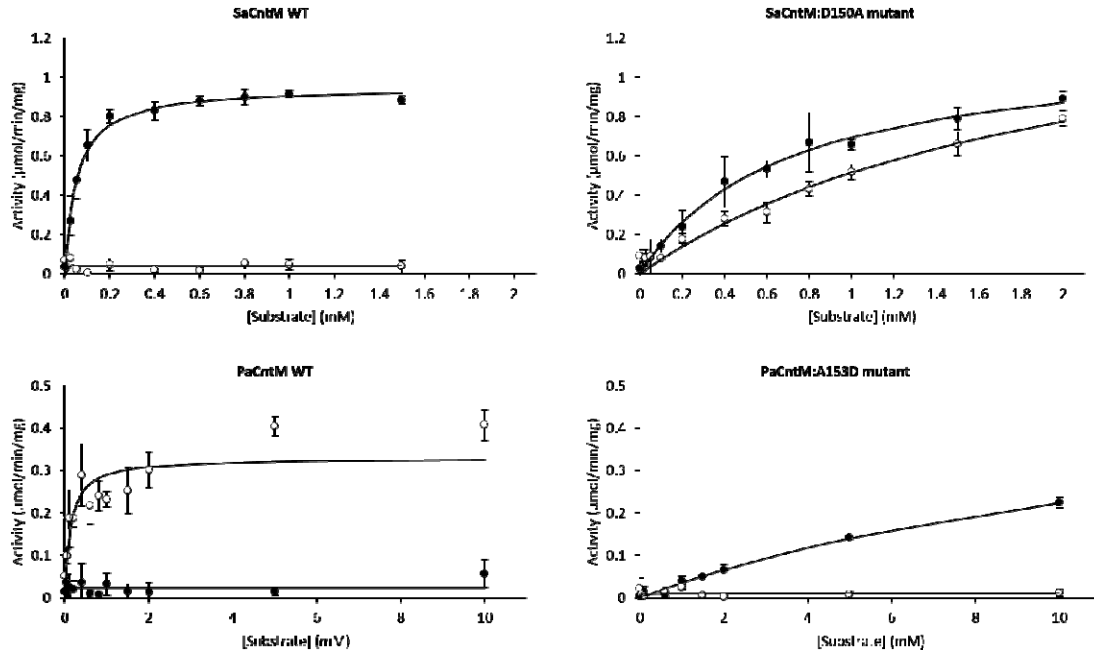
500

501

Protein	xNA vs yNA	K_m (μM)	K_i (mM)	k_{cat} (s^{-1})	k_{cat}/K_m ($\text{M}^{-1}\text{s}^{-1}$)
SaCntM	yNA	47 ± 9	2.3 ± 0.8	3.18 ± 0.25	67 584
SaCntM	xNA	23 ± 3	NA	1.67 ± 0.04	72 711
PaCntM	yNA	21 ± 7	2.4 ± 1.0	0.62 ± 0.06	29 618
PaCntM	xNA	54 ± 20	NA	0.16 ± 0.02	2 918

502 Table 1: Kinetic parameters of SaCntM and PaCntM activities established for a concentration range of
503 xNA and yNA with fixed concentrations of other substrates: 0.2 mM of NADPH and 1 mM of
504 pyruvate when evaluating SaCntM, and 0.2 mM of NADH and 1 mM of α -ketoglutarate when
505 evaluating PaCntM. The data and the standard errors associated with were generated by SigmaPlot
506 according to the Michaelis-Menten model with or without substrate inhibition. (NA: Not Applicable;
507 V_m : Maximum velocity; K_m : Michaelis constant; K_i : Inhibition constant; k_{cat} : Catalytic constant (or
508 turnover number); k_{cat}/K_m : Catalytic efficiency).

509



510

511 Figure 5: Activity profile of SaCntM (WT and D150A mutant) and PaCntM (WT and A153D mutant)
512 using variable concentrations of pyruvate (black circle) and α -ketoglutarate (white circle) with fixed
513 concentrations of others substrates: 0.2 mM of NADPH and xNA when evaluating SaCntM, and 0.2
514 mM of NADH and yNA when evaluating PaCntM. The data points are means of three replicates with
515 standard deviations. The fits are made using the Michaelis-Menten model.

516

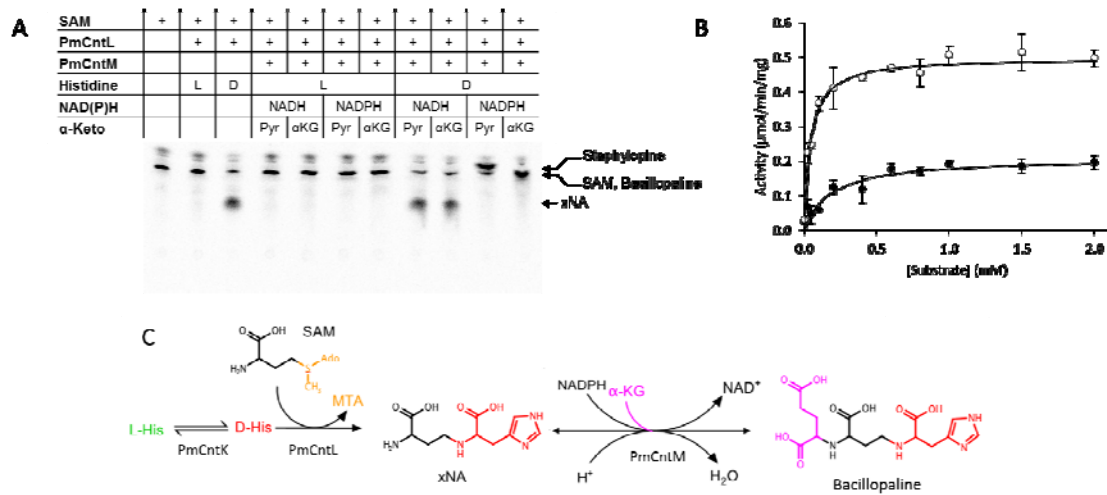
Protein	Pyruvate vs αKG	K_m (μM)	k_{cat} (s^{-1})	$k_{cat}/K_m(M^{-1}s^{-1})$
SaCntM	pyruvate	51 ± 6	1.00 ± 0.02	19 592
SaCntM	α KG	ND	0.04 ± 0.01	ND
SaCntM:D150A	pyruvate	$681 \pm 115^*$	$1.23 \pm 0.08^*$	$1\ 807^*$
SaCntM:D150A	α KG	$2\ 040 \pm 431^*$	$1.65 \pm 0.22^*$	809^*
PaCntM	pyruvate	ND	0.02 ± 0.01	N.D.
PaCntM	α KG	133 ± 39	0.27 ± 0.02	2 058
PaCntM:A153D	pyruvate	$14\ 986 \pm 2964^*$	$0.46 \pm 0.07^*$	31
PaCntM:A153D	α KG	ND	0.01 ± 0.01	ND

517 Table 2: Kinetic parameters of SaCntM (WT and D150A mutant) and PaCntM (WT or A153D
518 mutant) activities established for a concentration range of pyruvate and α KG with fixed concentrations
519 of other substrates: 0.2 mM of NADPH and xNA when evaluating SaCntM, and 0.2 mM of NADH
520 and yNA when evaluating PaCntM. The data and the standard errors associated with were generated
521 by SigmaPlot according to the Michaelis-Menten model. (ND: Not Determined). *Because the
522 maximum enzyme activity is not reached, these values are not well defined and must be taken with
523 caution.

524

525

526



527

528 Figure 6: Activity of CntL and CntM from *Paenibacillus mucilaginosus*. (A) TLC separation of
 529 reaction products incubating carboxyl- ^{14}C -labeled with purified enzyme (PmCntL and PmCntM) and
 530 various substrates (L-His (L) or D-His (D), pyruvate (Pyr) or α -ketoglutarate (α KG), NADH or
 531 NADPH). (B) Activity profile of PmCntM using variable concentrations of pyruvate (black circle) and
 532 α -ketoglutarate (white circle) with fixed concentrations of others substrates: 0.2 mM of NADPH and
 533 0.2 mM of xNA. The data points are means of three replicates with standard deviations. The fits are
 534 made using the Michaelis-Menten model. (C) Biosynthetic pathway for the assembly of bacillopaline
 535 from D-His, SAM and α -ketoglutarate.

536

Protein	Pyruvate vs αKG	K_m (μM)	k_{cat} (s^{-1})	k_{cat}/K_m ($M^{-1}s^{-1}$)
PmCntM	pyruvate	180 ± 39	0.18 ± 0.01	1 016
PmCntM	α KG	42 ± 5	0.44 ± 0.01	10 367

537 Table 3: Kinetic parameters of PmCntM activities established for a concentration range of pyruvate
538 and α KG with fixed concentrations of others substrates: 0.2 mM of NADPH and 0.2 mM of xNA. The
539 data and the standard errors associated with were generated by SigmaPlot according to the Michaelis-
540 Menten model.